The Effect of In Implantation on the Structural and Nano-Mechanical Properties of GaN

P. Kavouras[1*], J. Arvanitidis[1], E. Fournou[1], B. Kargas[1], M. Katsikini[2], E. C. Paloura[2], S. Ves[2], W. Wesch[3] and E. Wendler[3]

[1] *Department of Applied Sciences, Technological Educational Institute of Thessaloniki, 57400 Sindos, Greece*
[2] *Physics Department, Aristotle University of Thessaloniki, 54124 Thessaloniki, Greece*
[3] *Institut für Festkörperphysik, Friedrich-Schiller-Universität Jena, Max-Wien-Platz 1, Jena D-07743, Germany*

* *pkavo@physics.auth.gr*

In implantation of GaN is a promising method for the fabrication of InGaN/GaN nanostructures. The large scale implementation of this method requires the study of the effects induced by the implantation of In projectiles on the physical properties of GaN. In the present work, we study the structural and the mechanical properties, at the nano-scale, of n-type GaN grown on Al_2O_3 implanted with 700 keV In ions and fluences ranging from 5×10^{13} ions/cm^2 to 1×10^{16} ions/cm^2. The disorder degree of the films has been probed by means of Raman spectroscopy, while the mechanical properties were obtained by the quasi-static nano-indentation technique.

The Raman spectra were recorded in the backscattering geometry using a DILOR XY micro-Raman system equipped with a cryogenic charge coupled device (CCD) detector. For excitation, the 514.5 nm line of an Ar^+ laser was focused on the sample by means of a 100× objective lens with a laser power of ~5 mW. Mechanical properties were obtained by the Hysitron Ubi-1 Tribolab modular instrument. The nanomechanical characterization techniques applied gave quantitative results concerning the nanohardness value. Qualitative results about the elasto-plastic response and crack initiation were obtained by the shape of the load-unload curves.

The Raman spectra of the implanted GaN samples with varying In fluences are illustrated in figure 1 along with that of the as-grown material. For wurtzite GaN, factor group analysis predicts at Γ point the symmetry species $A_1+E_1+2B_1+2E_2$. The A_1, E_1 (which are polar and split into longitudinal, LO, and transverse optical, TO, components), and the two E_2 modes are Raman active, while the B_1 modes are silent [1]. In the backscattering geometry used here the two in-plane E_2 modes are favoured, observed in the as-grown sample at ~143 (E_2^1, Ga sublattice) and ~571 (E_2^2, N sublattice), while the totally symmetric along *c*-axis A_1(LO) Raman mode expected at ~739 cm^{-1} is completely damped due to plasmon-phonon coupling. The relatively narrow E_2^2 Raman peak (FWHM: ~5.1 cm^{-1}) reflects the good crystalline quality of the as-grown material. The frequency of the E_2^2 mode is strongly affected by biaxial stress induced in the GaN epilayer mainly due to the different thermal expansion coefficients of the epilayer (smaller) and the Al_2O_3 substrate (larger coefficient) and in the as-grown sample is upshifted by ~4.6 cm^{-1} compared to that in strain-free GaN [2]. From this blue shift, and taking into account that $\Delta\omega$(cm^{-1})= 6.2 σ(GPa) [3], we estimate a value of σ~ 0.74 GPa for the compressive biaxial strain in pristine GaN.

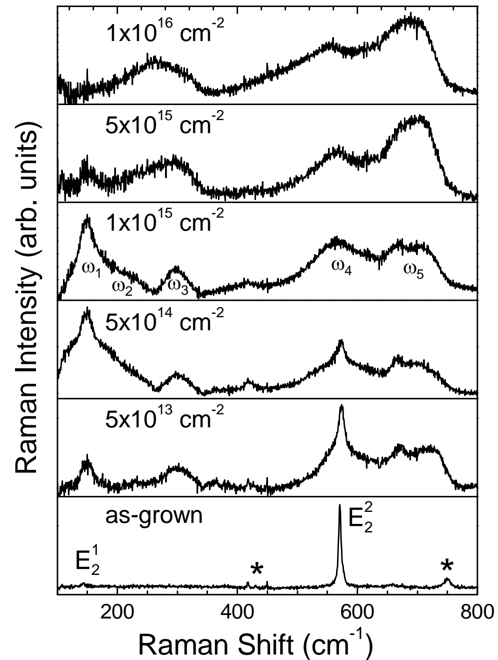

***Fig. 1**: Raman spectra -after background subtraction- of the In implanted (the numbers on the left refer to the In fluences) and the as-grown GaN samples. Asterisks mark peaks due to the Al_2O_3 substrate.*

In the implanted GaN with 5x10^{13} and 5x10^{14} cm^{-2} In fluences the E_2^2 peak attenuates and broadens significantly (FWHM: ~9.6 and ~11.2 cm^{-1}, respectively). Moreover, in both samples this Raman peak is blue shifted, compared to the as-grown sample, and is located at 573.3 cm^{-1} (σ~ 1.15 GPa) for the lower and at 572.6 cm^{-1} (σ~ 1.03 GPa) for the higher ion fluence, revealing that In implantation enhances initially the compressive strain of the GaN films, most probably due to the large atomic radius of In compared to that of Ga and N atoms. This is contrast to the situation encountered in the case of heavy ion implantation of GaN, where a partial stress relaxation is observed [4]. In these two samples, apart from

the E_2^2 peak new broad bands appear (marked by ω_1-ω_5 in the figure), rendering the Raman spectrum similar to that of amorphous GaN [5]. In amorphous materials, the *q*-selection rules -limiting Raman activity to zone-center modes- relax significantly, permitting every mode to contribute in the Raman spectrum. Thus, the spectrum reflects, in a certain degree, the phonon density of states of the material. In our case, the ω_1-ω_3 peaks could be attributed to the acoustic band of GaN dominated by the Ga atomic motions, while the ω_4 and the ω_5 peaks to the transverse and the longitudinal optic band, respectively dominated by the N atomic motions [6]. At higher fluences (5×10^{15} and 1×10^{16} cm^{-2}), the E_2^2 peak disappears, revealing the complete amorphization of GaN after implantation.

Table 1: *Nanohardness value of In implanted and the as-grown GaN samples.*

In fluence (cm^{-2})	H (GPa)	Structure
1×10^{16}	4.0±0.4	amorphous
5×10^{15}	5.5±0.5	amorphous
1×10^{15}	32.5±5.0	heavily damaged
5×10^{14}	36.5±4.0	heavily damaged
5×10^{13}	34.0±3.0	damaged
as-grown	28.5±3.5	wurtzite

The nanohardness value of In implanted samples together with that of the as-grown GaN sample are listed in Table 1. For fluences up to 1×10^{15} cm^{-2} the nanohardness value is increased with respect to that of the unimplanted GaN film. For higher fluences, an abrupt decrease in the nanohardness value was monitored. The errors shown in Table 1 represent the standard deviations obtained from five indentations. The respective indentation loads were high enough in order to produce indentation events with maximum depth approximately equal to half of the radius of curvature of the indenter tip, i.e. ≈ 60 nm.

Additionally, unimplanted GaN and implanted samples for fluences up to 1×10^{15} cm^{-2} showed normal Indentation Size Effect (ISE), while for higher fluences they showed reverse ISE. These results should be treated with caution, since the nanohardness values for indentation depths lower than half of the indenter tip radius of curvature can give rise to misleading results [7]. Normal ISE is connected to primarily elastically deformed films, while reverse ISE is connected to primarily plastic behavior. In this case, the material does not offer resistance or exhibit elastic recovery, but undergoes relaxation involving a release of the indentation stress away from the indentation site [8]. Study of the loading-unloading curves (figure 2) showed that for fluences up to 1×10^{15} cm^{-2} the behavior of the samples is indeed mainly elastic, with higher elastic recovery. In the above cases all load-unload curves can be bearly distinguished. For the two amorphized samples the unloading curve is markedly different and characteristic of primarily plastic behavior. As a result, it is possible that the markedly different nano-hardness values (not presented here), for shallower than 60 nm indentations, are a manifestation of an Indentation Effect.

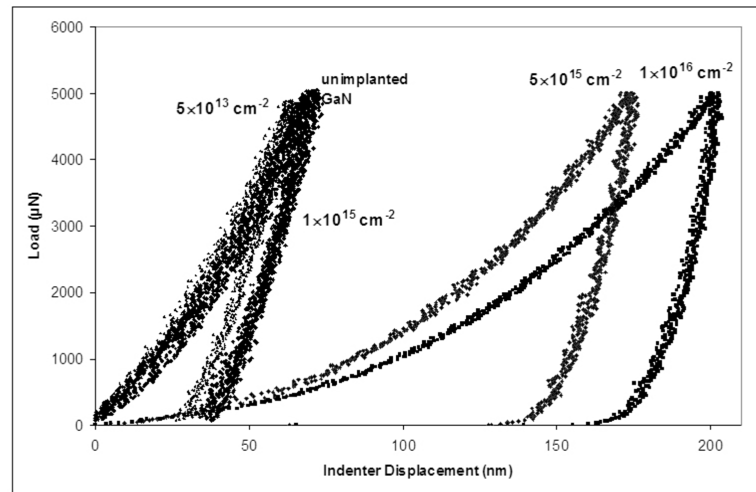

Fig. 2*: Load-unload curves of the In implanted and the as-grown GaN samples. The numbers in the diagram correspond to the In fluences in* cm^{-2}.

The analyses made by both Raman spectroscopy and Quazi-static nano-indentation techniques have given results that comply with each other, concerning the effect of In implantation. The combination of structural and mechanical response to In implantation was also compatible with the effect of heavy ion implantation on GaN films reported in previous studies [4,9].

[1] Zhang J. M., Ruf T., Cardona M., O. Ambacher, M. Stutzmann et al., Phys. Rev. B 56, 14399 (1997)
[2] Kisielowski C., Kruger J., Ruvimov S., Suski T., Ager III J.W. et al., Phys. Rev. B 54, 17745 (1996)
[3] Kozawa T., Kachi T., Kano H., Nagase H., Koide N. and Manabe K., J. Appl. Phys. 77 (1995) 4389
[4] Katsikini M., Arvanitidis J., Paloura E. C., Ves S., Wendler E. and Wesch W., Optical Materials 29, 1856 (2007)
[5] Bittar A., Trodahl H. J., Kemp N. T. and Markwitz A., Appl. Phys. Lett. 78, 619 (2001)
[6] Pollard W., J. Non-Cryst. Solids 283, 203 (2001)
[7] Fischer-Cripps A.C., Surf. Coat. Technol. 200, 4153 (2006)
[8] Sangwal K., Chem. Phys. 63, 145 (2000)
[9] Kavouras P., Komninou Ph. and Karakostas Th., Thin Solid Films 515, 3011 (2007)